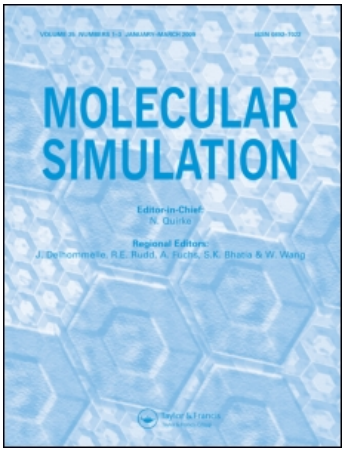

Molecular Simulation
Publication details, including instructions for authors and subscription information:
http://www.informaworld.com/smpp/title~content=t713644482

A Study of Conformational Equilibria in Chain Molecules. I. Liquid *n*-Butane

Haruhisa Hayashi[a]; Hideki Tanaka[a]; Koichiro Nakanishi[a]
[a] Division of Molecular Engineering, Graduate School of Engineering, Kyoto University, Sakyo-ku, Kyoto, Japan

To cite this Article Hayashi, Haruhisa , Tanaka, Hideki and Nakanishi, Koichiro(1993) 'A Study of Conformational Equilibria in Chain Molecules. I. Liquid *n*-Butane', Molecular Simulation, 9: 6, 401 — 415
To link to this Article: DOI: 10.1080/08927029308048270
URL: http://dx.doi.org/10.1080/08927029308048270

Molecular Simulation, 1993, Vol. 9(6), pp. 401-415
Reprints available directly from the publisher
Photocopying permitted by license only

A STUDY OF CONFORMATIONAL EQUILIBRIA IN CHAIN MOLECULES. I. LIQUID *n*-BUTANE

HARUHISA HAYASHI, HIDEKI TANAKA AND KOICHIRO NAKANISHI

Division of Molecular Engineering, Graduate School of Engineering, Kyoto University, Sakyo-ku, Kyoto 606-01, Japan

(*Received June 1992, accepted June 1992*)

We have performed molecular dynamics simulations for liquid *n*-butane in order to understand liquid structures in terms of both inter- and intra-molecular interactions. Each n-butane molecule consists of four sites interacting with LJ potential and only a dihedral angle is taken into account as the internal degree of freedom. The population of *gauche* conformations with respect to the ideal gas state is found to increase in the liquid state. To investigate how the intermolecular interaction affects the dihedral angle distribution, we also adopt the repulsive LJ potential (RLJ) model. It is found that the nearest neighbor packing of the methyl and/or methylene groups can be approximately represented by using only the repulsive interaction. From the dihedral angle distribution, however, the rate of the shift of RLJ model to *gauche* is larger than that of LJ model and the attractive force also plays a significant role in the conformational equilibrium.

KEY WORDS: Molecular dynamics simulation, *n*-butane, Dihedral angle, Intermolecular interaction, Intramolecular interaction.

INTRODUCTION

Many investigations for liquids and liquid mixtures composed of rigid molecules have been carried out for the last three decades. The structure and dynamics of classical liquids are now better understood due to recent developments in computer simulation. Little attention has, however, been paid to the molecules having internal degrees of freedom such as *n*-butane with the dihedral angle, since a complicated nature of the liquid structures arising both from intermolecular and intramolecular interactions prevented us from understanding the roles played by the internal degrees of freedom.

It is believed that the distribution of the dihedral angle of *n*-butane molecule in the liquid state is different from that in the ideal gas. However, the origin of this difference is not clear. The distribution of the dihedral angle is a measure of the effect on the internal degree of freedom, arising from the intermolecular interaction. Historically, this distribution function in the condensed phase was discussed in terms of the random distribution or the short range packing effect. The former view proposed by Flory [1] was based on the consideration that the distribution is dominated by random packing, and therefore, it should be the same as that in the ideal gas. On the other hand, statistical mechanical theory predicted that the distribution shifted to the *gauche* in favor of the short range packing. In fact, various methods such as the packing fraction theory, superposition approximation, and the two cavity model calculation have been proposed to evaluate the

distribution of the dihedral angle. According to these approximate methods, an increase in the population of the *gauche* conformation is estimated to be as large as 10% [2]. In a more realistic treatment with the reference interaction-site model (RISM) by Pratt and Chandler [3, 4], the increase is 7%. The recent computer simulation studies [5, 6, 7, 8] support this latter view derived from the statistical mechanical theory. However, the results are likely to be dependent on the models used, the simulation time, the existence of the attractive forces, and other simulation conditions. Therefore, we will adopt n-butane as the simplest molecule, in which only a single internal degree of freedom is included and other stretching and bending vibrational motions are ignored, and examine the effect of the attractive forces on the dihedral angle distribution for n-butane by the molecular dynamics (MD) simulations in the present study.

2. MODEL AND POTENTIAL

Since we pay attention to the torsional motion of the dihedral angle, both intra and intermolecular interactions are taken into account. Our model for n-butane is the same as that used by Ryckaert and Bellemans [9]. Each *n*-butane molecule consists of four interaction sites centered on each carbon atom having the same mass ($m = 2.408 \times 10^{-23}$ g). All the hydrogen atoms of n-butane are neglected. The site-site distance is fixed at 1.53 Å and the bond angles are also fixed at 109.47°.

The intramolecular conformation of n-butane is defined by the dihedral angle, α, ($-180° < \alpha \leqslant +180°$) and the torsional potential is given as a function of α by

$$\nu^{DIH}(\alpha)/k_B = \{+1.116 + 1.462\cos\alpha - 1.578\cos^2\alpha - 0.368\cos^3\alpha + 3.156\cos^4\alpha - 3.788\cos^5\alpha\} \times 10^3\,\mathrm{K} \tag{1}$$

(k_B = Boltzmann's constant). This intramolecular potential has been proposed by Scott and Scheraga on the basis of IR and Raman spectroscopic measurements and the *ab-initio* calculations for an n-butane molecule in vacuum [10, 11]. The potential energy for *trans* conformation ($\alpha = 0°$) is set equal to 0 kJ mol^{-1} and that for $\pm$*gauche* conformation ($\alpha = \pm 120°$) is 2.93 kJ mol^{-1}. The potential barrier from *trans* to $\pm$*gauche* is 12.35 kJ mol^{-1}.

The site-site intermolecular potential is described by the Lennard-Jones 12-6 potential with a switching-function $\mathcal{SF}(R)$ [12] (we call this the LJ-model).

$$\nu^{\mathcal{SF}\text{-LJ}}(\mathbf{r}, \mathbf{r}') = \mathcal{SF}(R) \cdot \sum_{i,j} \nu^{\mathrm{LJ}}(r_{ij}) \tag{2}$$

$$\mathcal{SF}(R) = \begin{cases} 1 & , \quad (R < r_d) \\ \dfrac{(R-r_c)^3}{(r_d-r_c)^5}\{10(R-r_d)^2 + (R-r_c)^2 - 5(R-r_c)(R-r_d)\}, & (r_d \leqslant R < r_c) \\ 0 & , \quad (r_c \leqslant R) \end{cases} \tag{3}$$

$$v^{LJ}(r) = 4\varepsilon\left\{\left(\frac{\sigma}{r}\right)^{12} - \left(\frac{\sigma}{r}\right)^{6}\right\} \tag{4}$$

where R stands for the separation of the centers of mass, $\mathbf{r}$ (also $\mathbf{r}'$) denotes the Cartesian coordinates of all atoms on each molecule, r_{ij} is the distance between i and j sites. Size parameter σ and energy parameter ε are 3.923 Å and 72 K, respectively.

In the present MD calculation, all the n-butane molecules have initially the *trans* conformation ($\alpha = 0°$) and their orientations are random. Initial temperatures and densities are set equal to the experimentally observed values of liquid n-butane (system A: 200 K, $\rho^* = 0.419$; system B: 291 K, $\rho^* = 0.365$)

Table 1 Conditions of MD simulations for *n*-butane interacting LJ and RLJ potential. The temperature, energies and the percentage of *trans* state (X^T) are also given. The temperature T, the density ρ^* are in Kelvin, LJ reduced unit, respectively. The unit of energy is kJ/mol.

	System	Average Temp. (K)	Total Energy	Potential Energy	Intra Energy	X^T (%) (dev.)
LJ-A	T = 200.00 K $\rho^* = 0.419$	192.79	−14.763	−20.372	+1.685	73.995 (3.826)
LJ-B	T = 291.00 K $\rho^* = 0.365$	279.21	−8.228	−16.352	+2.521	63.842 (3.771)
RLJ-A	T = 200.00 K $\rho^* = 0.419$	194.89	+10.499	+4.828	+1.885	67.581 (3.142)
RLJ-B	T = 291.00 K $\rho^* = 0.365$	286.23	+13.446	+5.118	+2.729	56.875 (3.603)

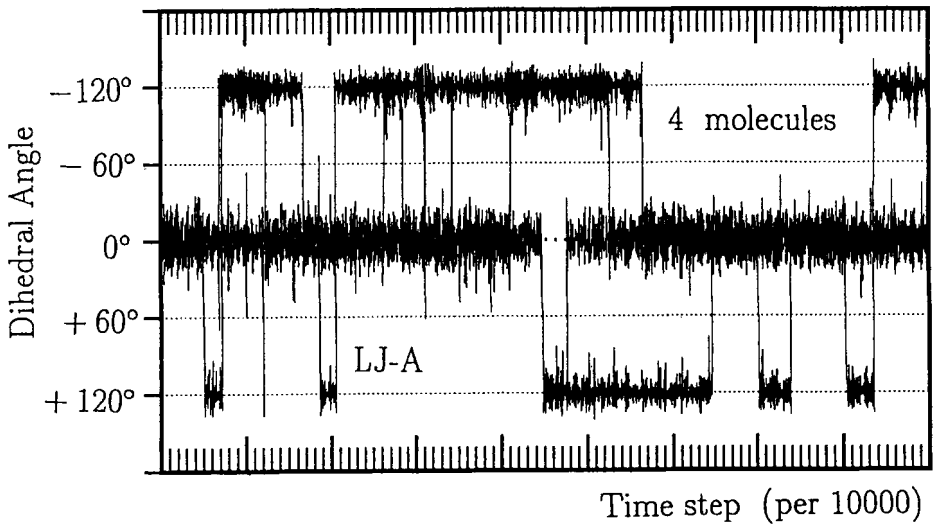

Figure 1 The time evolution of the dihedral angle of selected four molecules for 1737 ps: (A) system LJ-A (T = 192.79 K and $\rho^* = 0.419$).

[9]. Equations of motion are solved by the Verlet method [13] and the constraints of bond angles and length are treated by the Shake algorithm [14]. A time step, Δt, for the integration of equations of motion is 1.93×10^{-15} sec. 108 n-butane molecules are confined in a cubic cell imposing the periodic boundary condition and the systems in the MD simulation correspond to the NEV-ensemble.

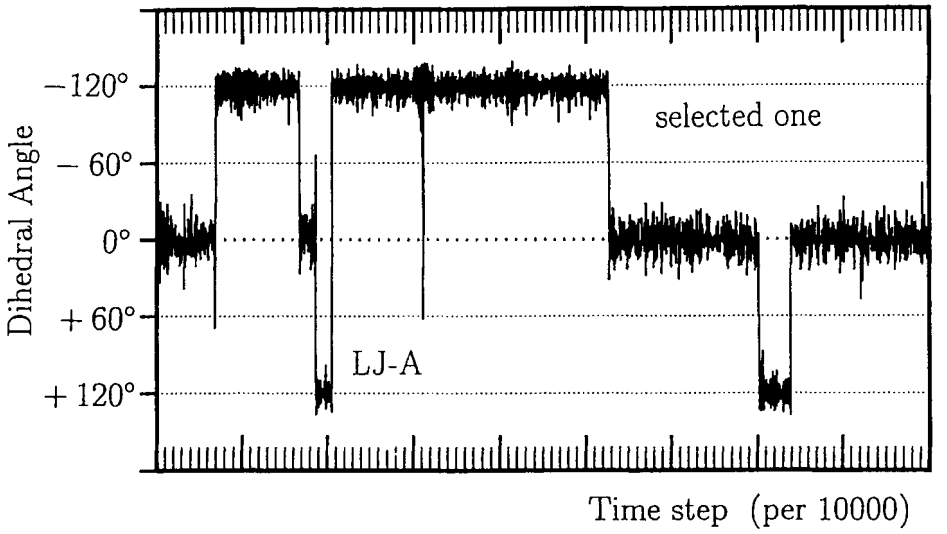

Figure 2 The time evolution of the dihedral angle of selected one molecule for 1737 ps: (A) system LJ-A (T = 192.79 K and $\rho^* = 0.419$).

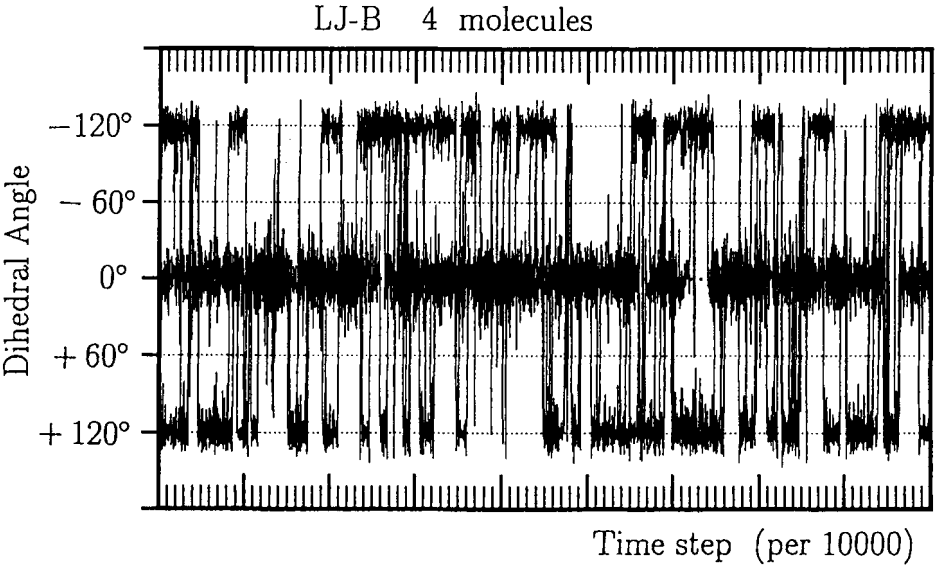

Figure 3 The time evolution of the dihedral angle of selected four molecules for 1737 ps: (B) system LJ-B (T = 279.21 K and $\rho^* = 0.365$).

The MD simulation is extended to 900,000 time steps (1737 ps) for each system. This simulation time is long enough to evaluate the dihedral angle distribution with better statistics than that of previous studies [6, 9].

In order to understand how the attractive part of the LJ interaction from other molecules affects the dihedral angle distribution, another potential, repulsive LJ (RLJ) model which has only the repulsive part is also examined. The repulsive part of the potential was evaluated by adopting the Weeks-Chandler-Andersen (W.C.A.) type separation [15].

3. RESULTS AND DISCUSSION

The energy and dihedral angle distribution obtained from the present MD simulations are given in Table 1. The *trans* conformation is defined by the region of the dihedral angle α, $-60° < \alpha < +60°$, and the *gauche* conformation by that of $-180° < \alpha \leqq -60°$ and $+60° \leqq \alpha \leqq +180°$. X^T and X^G $(=1-X^T)$ stand for the fraction of *trans* and *gauche* conformational populations, respectively. Standard deviations are also given in the parentheses of this table. The deviations are calculated by dividing whole simulation run into several blocks comprising consecutive 10000 steps (19.3 ps). In the RLJ model, the total energy of the system is positive. This is simply because the RLJ potential does not have the attraction term and is positive in all regions.

3.1 Time evolution of the dihedral angle

We can obtain the time evolution of the dihedral angles of individual molecules in the LJ model. Figures 1 to 4 show the typical examples of the time evolution of the

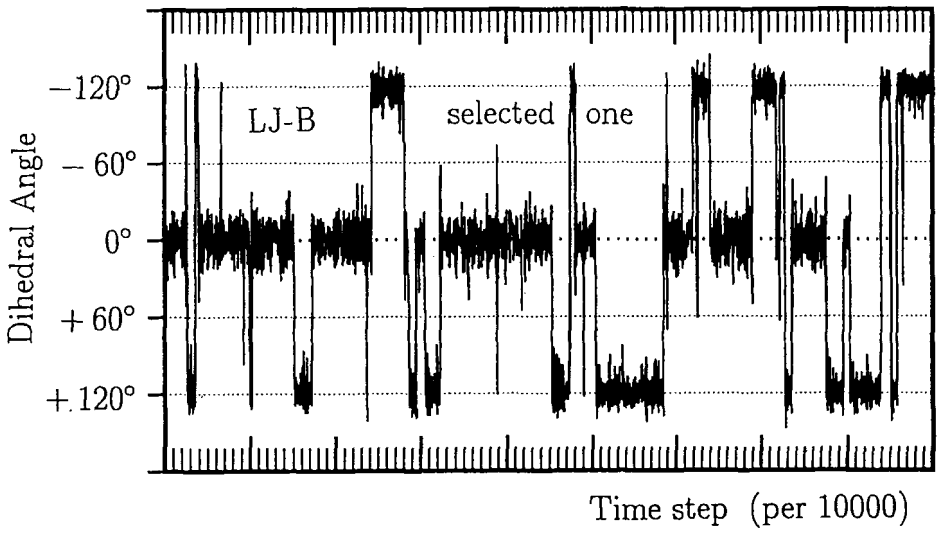

Figure 4 The time evolution of the dihedral angle of selected one molecule for 1737 ps: (B) system LJ-B (T = 279.21 K and $\rho^* = 0.365$).

dihedral angles for the LJ model. The higher the temperature is, the more frequently the rotation of the dihedral angle in *n*-butane molecule takes place. Moreover, various patterns of rotation are observed; *trans* → ±*gauche* transformation, ±*gauche* → *trans* formation, and ±*gauche* → ∓*gauche* direct transformation. In the case of RLJ model, we can obtain the similar results to that of LJ model, and they are not shown here.

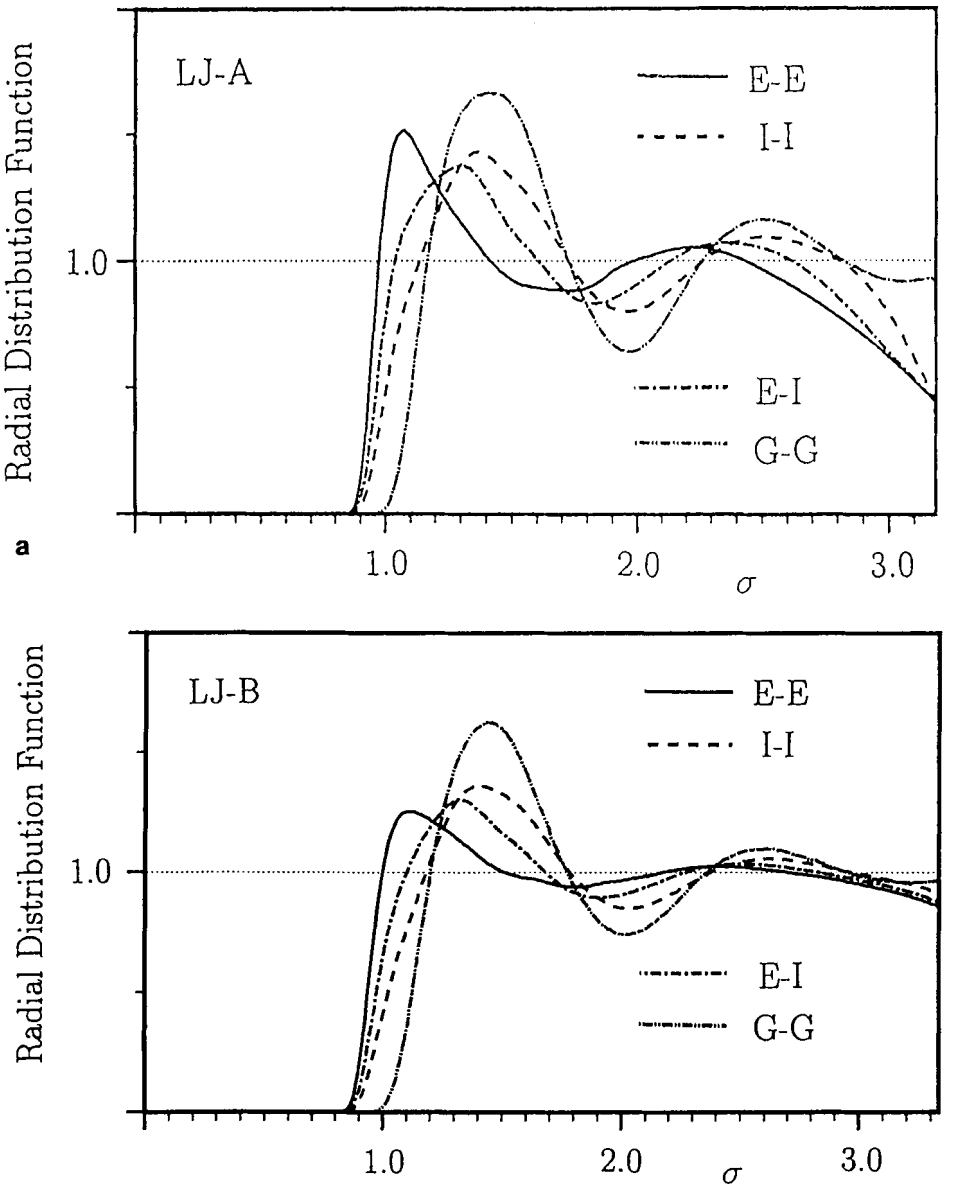

Figure 5 Site-site radial distribution functions for the LJ model n-butane. End-End (E-E; solid line), Inner-Inner (I-I; dashed line), End-Inner (E-I; dash-dot line), centers of mass (G-G; dash-double dots line) RDF for (A) System LJ-A and (B) System LJ-B.

3.2 Radial Distribution

Although the temperatures for both the LJ and the RLJ systems are different slightly with each other, the difference in the radial distribution function (RDF) arising from the temperature difference is expected to be small. No correction due

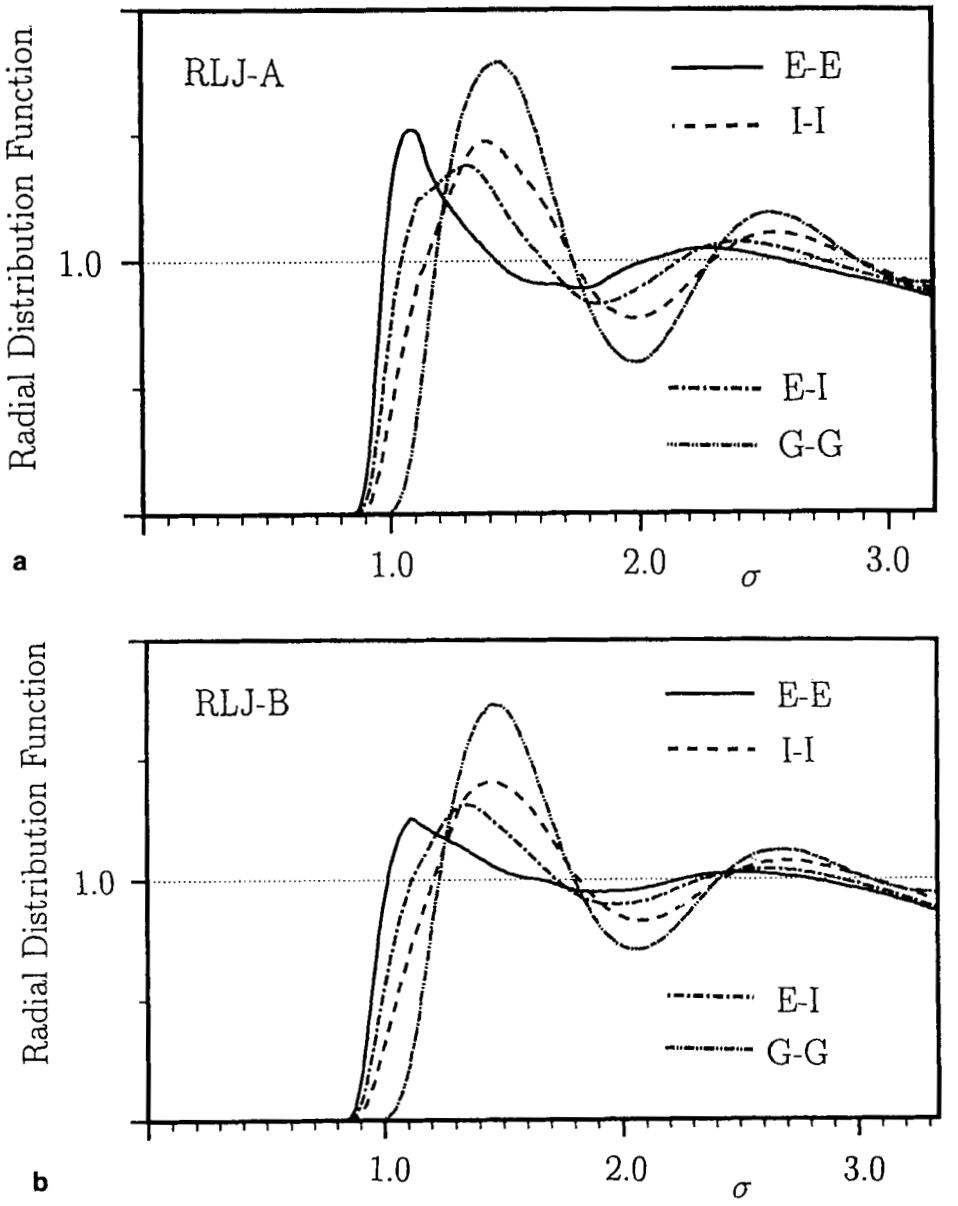

Figure 6 Site-site radial distribution functions for the RLJ model n-butane. The solid line, dashed line, dash-dot line and dash-double dots line show the End-End (E-E), Inner-Inner (I-I), End-Inner (E-I) and centers of mass (G-G) RDF respectively. (A) System RLJ-A and (B) System RLJ-B.

to the difference is made for RDF's, when they are compared. Figures 5 and 6 show the End-End (E-E), Inner-Inner (I-I), End-Inner (E-I), and centers of mass (G-G) RDF's for the LJ and the RLJ models, respectively. As seen from these figures, the first peak of G-G RDF in either system is rather broad compared with the site-site RDF's. This is a contrast to the case of small diatomic molecule such as nitrogen. This is caused by the relatively large center of mass motions of individual molecules. Those are, in turn, due partly to the large change of dihedral angles.

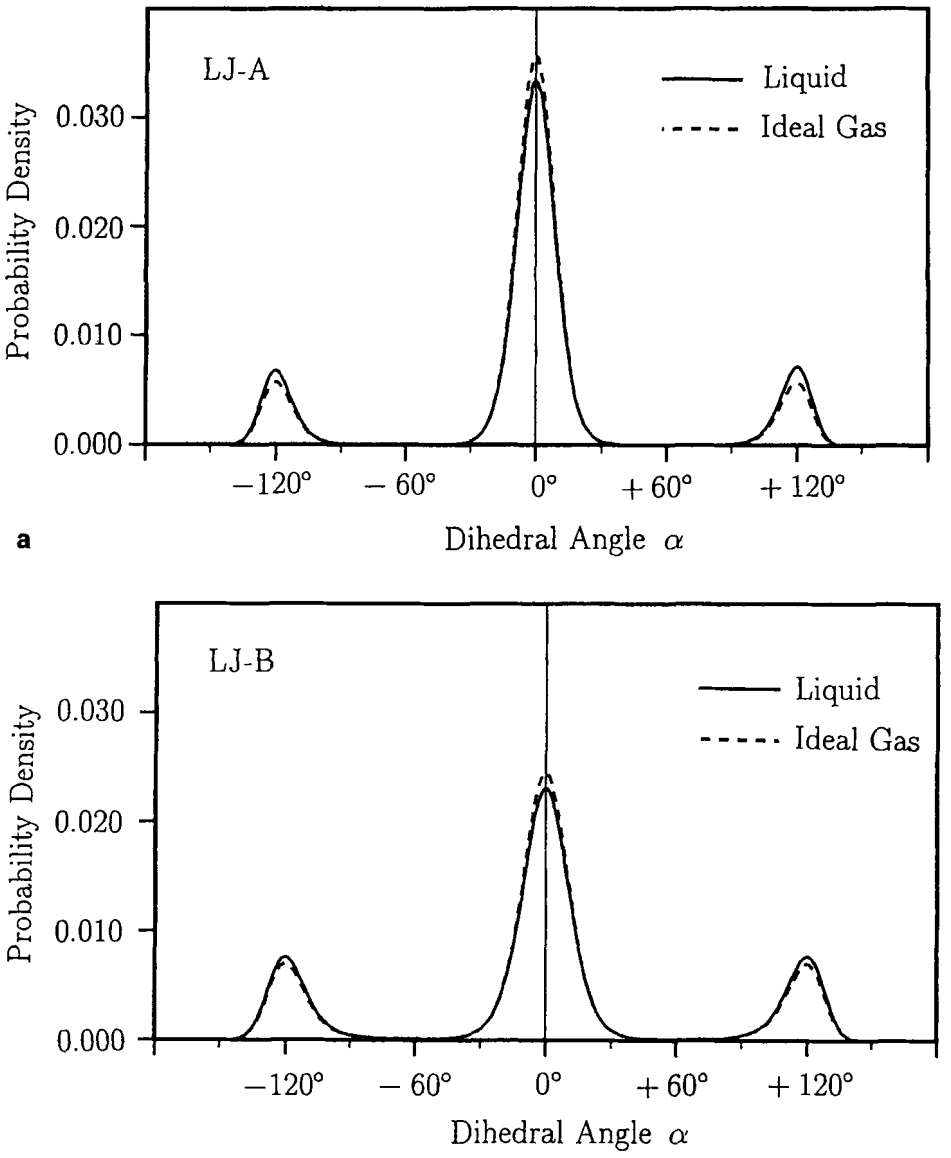

Figure 7 The distribution of the dihedral angle in the LJ model in liquid phase (solid line) and in the ideal gas state at the same temperature (dashed line). (A) System LJ-A and (B) System LJ-B.

Table 2 Dihedral angle distributions for both models. The temperature T, the density ρ^* are in Kelvin, LJ reduced unit, respectively. X^T and X^G $(=1-X^T)$ are the ratios of *trans* state and *gauche* state population respectively. ΔX stands for the conformational equilibrium shifts toward the *gauche* form $(\Delta X = X^G_{liquid} - X^G_{ideal\ gas} = -(X^T_{liquid} - X^T_{ideal\ gas}))$. The unit is percent (%).

LJ model		System LJ-A (T = 192.79 K, $\rho^* = 0.419$) X^T : X^G	System LJ-B (T = 279.21 K, $\rho^* = 0.365$) X^T : X^G
Ideal gas	(dashed line)	78.321 : 21.679	67.028 : 32.972
Liquid state	(solid line)	73.995 : 26.005	63.842 : 36.158
ΔX		4.326	3.158
RLJ model		**System RLJ-A (T = 194.89 K, $\rho^* = 0.419$) X^T : X^G**	**System RLJ-B (T = 286.23 K, $\rho^* = 0.365$) X^T : X^G**
Ideal gas	(dashed line)	77.980 : 22.020	66.328 : 33.672
Liquid state	(solid line)	67.581 : 32.419	56.875 : 43.125
ΔX		10.399	9.453

Comparing the RLJ model with the LJ model, only a small difference is seen in RDF. The peak positions for the RLJ model shift slightly to long distance direction over all distance ranges. This is explained simply by the fact that there is no attractive interaction in RLJ model. It is found that, except for a small shift in RDF's, there is no significant difference in the short range structures of system between both models [16].

3.3 Distribution of the dihedral angle

The distribution of the dihedral angle calculated from the MD simulations is shown in Figures 7 (LJ model) and 8 (RLJ model) and also in Table 2. It is found that X^G_{liquid} $(=1-X^T_{liquid})$ in the liquid state increases from that in the ideal gas state $(X^G_{ideal\ gas})$. The conformational equilibria shift toward the *gauche* form due to the presence of other molecules. This shift ΔX,

$$\Delta X = X^G_{liquid} - X^G_{ideal\ gas} = -(X^T_{liquid} - X^T_{ideal\ gas}) \tag{5}$$

depends on the simulation conditions and is between 3 and 5% in the case of the LJ model.

For the RLJ model, the increase in ΔX is almost 10%, which should be compared with that obtained from theoretical calculation using a fused hard-sphere system [4]. Then, we try to separate the origin of the distribution into two contributions as

$$\mathcal{V}^{DIH}_{liquid}(\alpha) = \mathcal{V}^{DIH}_{ideal\ gas}(\alpha) + \mathcal{W}^{DIH}(\alpha), \tag{6}$$

where $\mathcal{V}^{DIH}_{liquid}(\alpha)$ is calculated from the dihedral angle distribution as

$$\mathcal{V}^{DIH}_{liquid}(\alpha) = -k_B T \ln(X_{liquid}(\alpha)). \tag{7}$$

The first term in the right-hand side of equation (6) is a torsional potential in the ideal gas and the second term is the indirect interaction due to the intermolecular interactions.

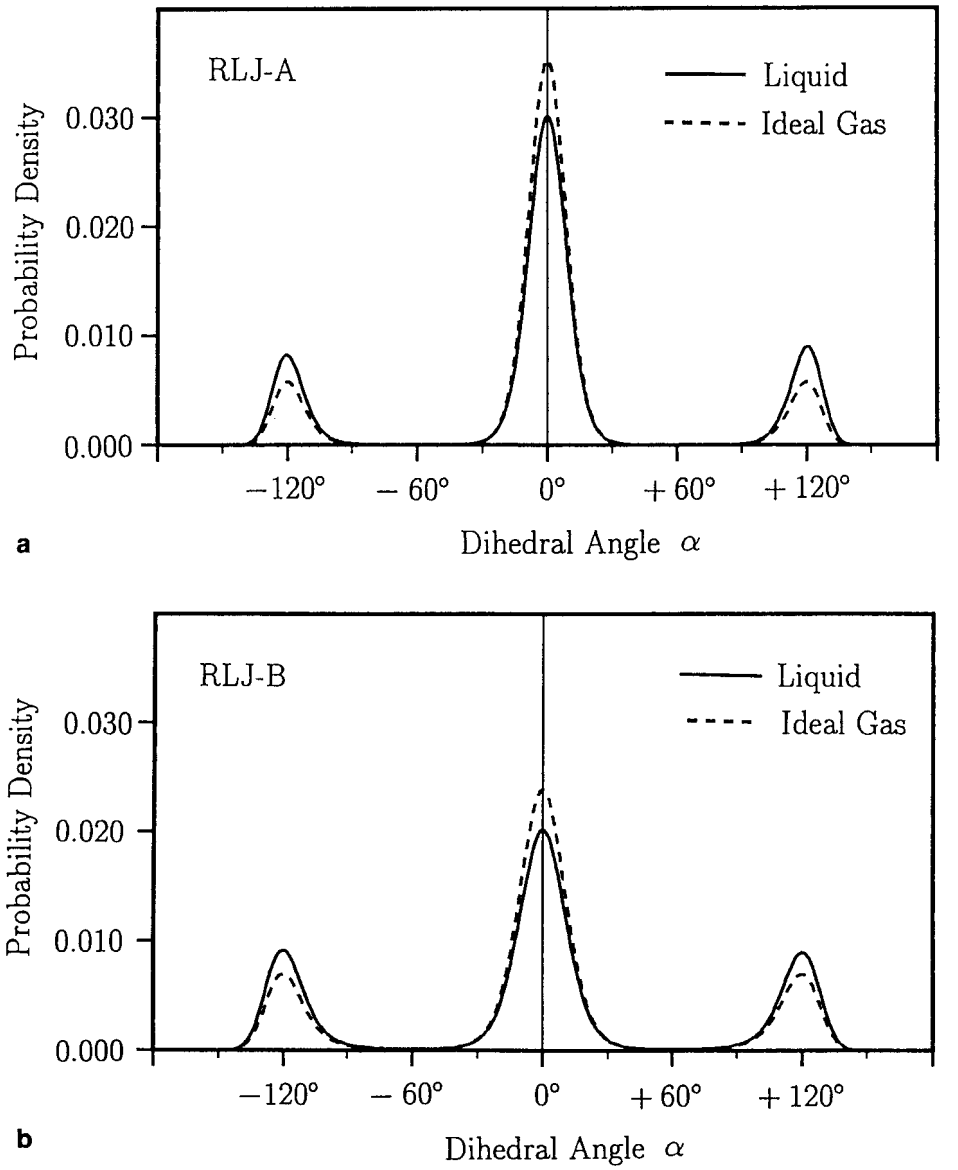

Figure 8 The distribution of the dihedral angle in the RLJ model, in liquid phase (solid line) and in the ideal gas state at the same temperature (dashed line). (A) System RLJ-A and (B) System RLJ-B.

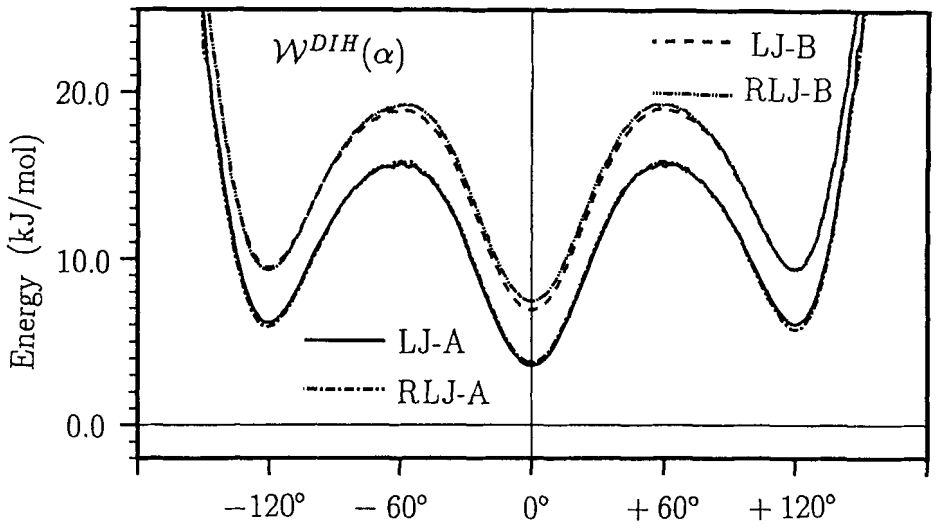

Figure 9 The effective potential in the liquid phase for the System LJ-A (solid line), LJ-B (dashed line), RLJ-A (dash-dot line) and RLJ-B (dash-double dots line) n-butane.

In Figure 9 is shown the torsional potential in the liquid state, as a function of the dihedral angle in the LJ and the RLJ models. As seen from this figure, there is a small difference between two systems for which conditions other than the intermolecular potential function are the same. In order to make the discussion clearer when these dihedral angle distributions are compared, we define the relative magnitude of the torsional potential as

$$\mathcal{V}'^{DIH}_{liquid}(\alpha) = -k_B T \ln(X_{liquid}(\alpha)/X_{liquid}(0)). \tag{8}$$

The solvent induced contribution term $\mathcal{W}'^{DIH}(\alpha)$ is shown as

$$\mathcal{W}'^{DIH}(\alpha) = \mathcal{V}'^{DIH}_{liquid}(\alpha) - \mathcal{V}^{DIH}_{ideal\ gas}(\alpha). \tag{9}$$

In Figures 10 and 11 are shown two contributions to the dihedral angle distribution ($\mathcal{V}'^{DIH}_{liquid}(\alpha)$ and $\mathcal{W}'^{DIH}(\alpha)$) in the LJ and the RLJ models, repsectively. The induced term ($\mathcal{W}'^{DIH}(\alpha)$) is also shown in Figure 12. On account of intermolecular interactions, the *gauche* conformation in the liquid state is more stabilized than that in the gas phase, relatively. This tendency for the molecule to become "fold" or small in size is fairly dependent upon the attractive part of the potential.

4. SUMMARY

Conformational equilibria for *n*-butane have been investigated by MD simulations. Intermolecular interactions give rise to the shift of the equilibrium toward the *gauche* conformation. This is explained in terms of a simple packing effect in the condensed phase. Our results for the LJ model agree qualitatively with those from

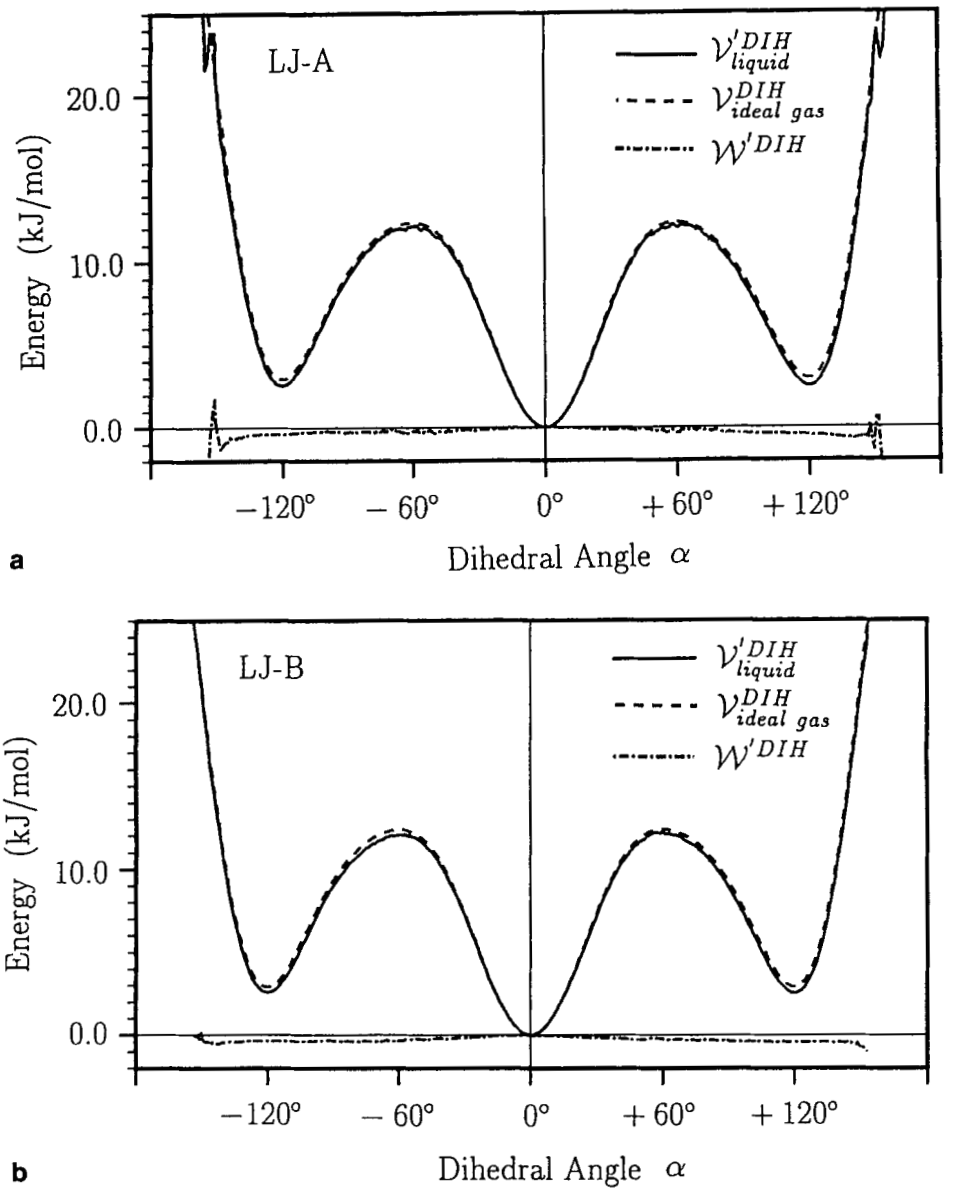

Figure 10 The dihedral angle potential for the LJ model of n-butane in (A) System LJ-A and (B) System LJ-B. The solid line shows the relative induced potential in the liquid phase. The dashed line represents Scott-Scheraga's potential.

recent computer simulations [5, 6, 7, 8]. However, the magnitude of the shift in the dihedral angle distribution depends on the models used and the conditions of simulation.

The following results are obtained from the repulsive LJ model calculation. From the result of RDF's, the structure of liquid *n*-butane can be to great extent represented only by the repulsion part of the potential. However, comparing the

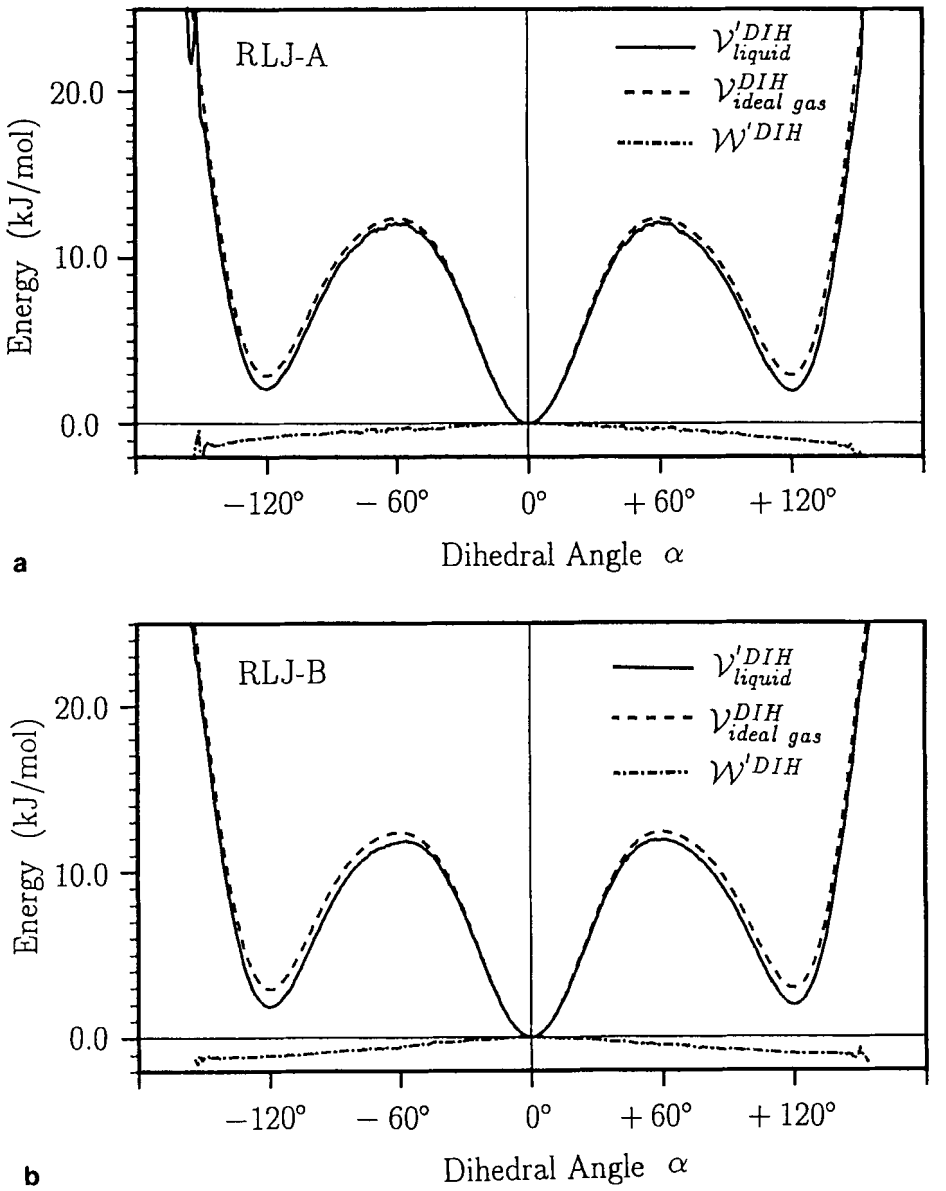

Figure 11 The dihedral angle potential for the RLJ model of n-butane in (A) System RLJ-A and (B) System RLJ-B. The solid line is the relative induced potential in the liquid phase. The dashed line represent Scott-Scheraga's potential.

dihedral angle distribution of the RLJ model with that of the LJ model, the shift is more enhanced in the system of molecules interacting via a repulsive interaction only in place of the LJ interaction. The shift was 7% in the RISM calculation, where *n*-butane was approximated to a fused hard-sphere [4]. This value is in good correspondence with that obtained from our simulations for the RLJ systems. Therefore, the whole liquid structures including the dihedral distribution are

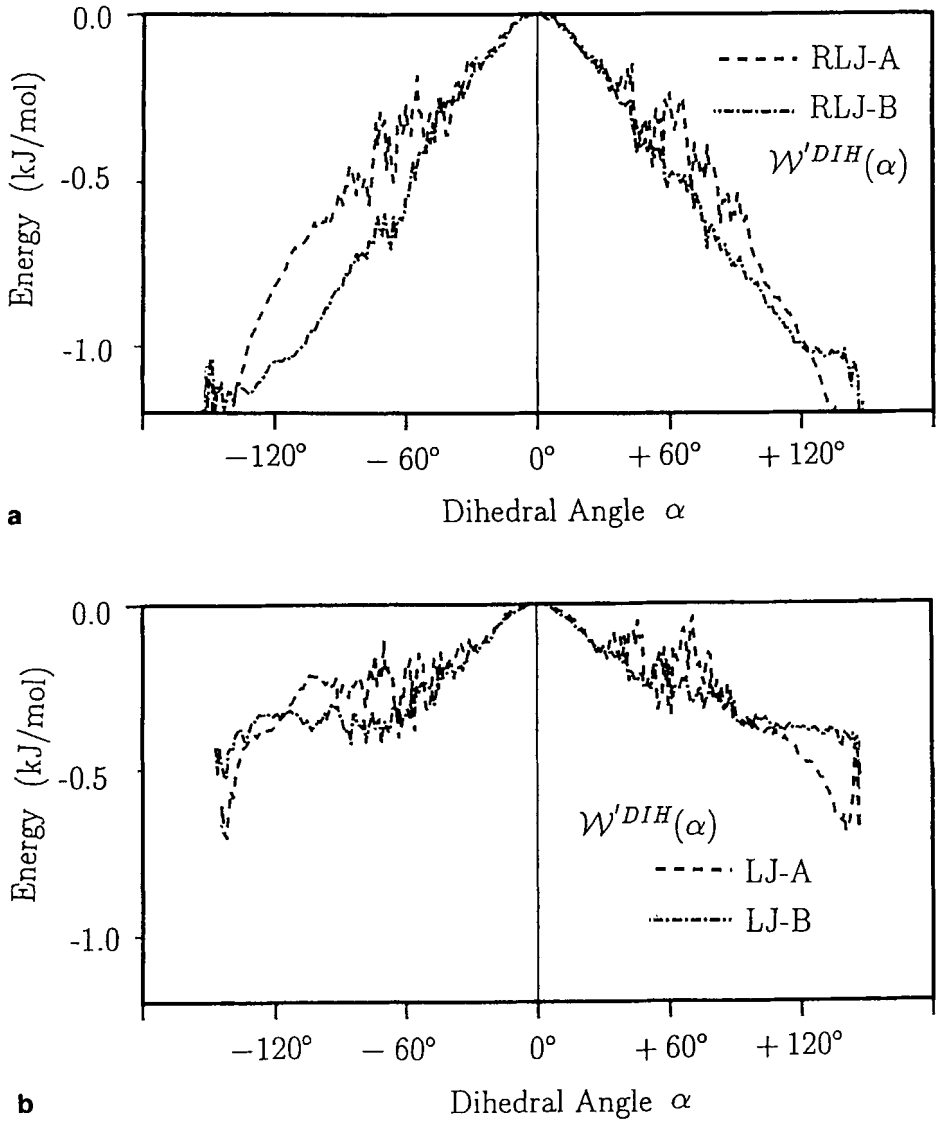

Figure 12 The solvent induced potential $\mathcal{W}'^{DIH}(\alpha)$ for (A) LJ model and (B) RLJ model.

sensitive to the attractive part of the intermolecular interaction as well as the repulsive part.

Acknowledgements

The authors are grateful to the Computer Center, Institute for Molecular Science and the Data Processing center, Kyoto University for the use of facilities.

References

[1] P.J. Flory, *Statistical Mechanics of Chain Molecules*, (Wiley-Interscience, New York, 1969).

[2] W.L. Jorgensen, "Internal rotation in liquid 1,2-dichloroethane and n-butane", *J. Am. Chem. Soc.* **103**, 677 (1981); "Pressure dependence of the structure and properties of liquid n-butane", *J. Am. Chem. Soc.* **103**, 4721 (1981).

[3] D. Chandler and L.R. Pratt, "Statistical mechanics of chemical equilibria and intramolecular structures of nonrigid molecules in condensed phases", *J. Chem. Phys.* **65**, 2925 (1976); L.R. Pratt and D. Chandler, "Theory of the hydrophobic effect", *J. Chem. Phys.* **67**, 3683 (1977).

[4] L.R. Pratt, C.S. Hsu and D. Chandler, "Statistical mechanics of small chain molecules in liquids. I. Effects of liquid packing on conformational structures", *J. Chem. Phys.* **68**, 4202 (1978); C.S. Hsu, L.R. Pratt and D. Chandler, "Statistical mechanics of small chain molecules in liquids. II. Intermolecular pair correlations for n-butane", *J. Chem. Phys.* **68**, 4213 (1978).

[5] R. Edberg, D.J. Evans and G.P. Morris, "Constrained Molecular Dynamics: Simulations of liquid alkanes with a new algorithm", *J. Chem. Phys.* **84**, 6933 (1986); "Conformational kinetics in liquid butane by nonequilibrium Molecular Dynamics", *ibid.* **87**, 5700 (1987).

[6] P.A. Wielopolski and E.R. Smith, "Dihedral angle distribution in liquid *n*-butane: Molecular Dynamics simulations", *J. Chem. Phys.* **84**, 6940 (1986).

[7] E. Enciso, J. Alonso, N.G. Almarza and F.J. Bermejo, "Statistical mechanics of small chain molecular liquids. I. Conformational properties of modeled n-butane", *J. Chem. Phys.*, **90**, 413 (1989); "Statistical mechanics of small chain molecular liquids. II. Structure and thermodynamic properties of modeled n-butane liquid", *ibid.* **90**, 422 (1989).

[8] D. Brown and J.H.R. Clarke, "A direct method of studying reaction rates by equilibrium Molecular Dynamics: Application to the kinetics of isomerization in liquid n-butane", *J. Chem. Phys.* **92**, 3062 (1990).

[9] J.P. Rychaert and A. Bellemans, "Molecular Dynamics and liquid alkanes", *Discuss. Faraday Soc.*, **66**, 95 (1978).

[10] R.A. Scott and H.A. Scheraga, "Conformation analysis of macromolecules. II. The rotational isomeric states of the normal hydrocarbons", *J. Chem. Phys.* **44**, 3054 (1966).

[11] P.B. Woller and E.W. Garbisch, Jr., "The conformational analysis of n-butane", *J. Am. Chem. Soc.*, **94**, 5310 (1972).

[12] I. Ohmine, H. Tanaka and P.G. Wolynes, "Large local energy fluctuations in water. II. Cooperative motions and fluctuations", *J. Chem. Phys.* **89**, 5852 (1988).

[13] M.P. Allen and D.J. Tildesley, *Computer simulation of liquids*, (Oxford University Press, New York, 1987).

[14] J.P. Ryckaert, G. Ciccotti and H.J.C. Berendsen, "Numerical integration of the Cartesian equations of motion of a system with constraints: Molecular Dynamics of n-alkanes", *J. Comput. Phys.* **23**, 327 (1977).

[15] J.D. Weeks, D. Chandler and H.C. Andersen, "Role of repulsive force in determining the equilibrium structure of simple liquids", *J. Chem. Phys.*, **54**, 5237 (1971).

[16] N.G. Almarza and E. Enciso *et al.*, "Monte Carlo simulations of liquid n-butane", *Mol. Phys.*, **70**, 485 (1990).